Journal of Renewable Energy and Sustainable Development (RESD) Volume 11, Issue 2, December 2025 - ISSN 2356-8569
http://dx.doi.org/10.21622/RESD.2025.11.2.1445

Received: 06 July 2025 Accepted: 11 August 2025 Published: 02 September 2025

Experimental Investigation of Axial-Flow Turbine Performance Using Water and Oil: Effects of Rotation Speed, Blade Count, and Oil Pre-Heating

Mays Subhi Sadeq [1*], and Muna S. Kassim [2]

[1*] AL-Mustansiriyah University, College of Engineering, Mechanical Engineering Department, Baghdad, Iraq
Ministry of Electricity, Modern Energy Center, Baghdad, Iraq

[2] National Investment Commission, Republic of Iraq

mayssubhi112@gmail.com, muna.kassim@mustansiriyah.edu.iq

Abstract

This experimental research looks at the hydraulic performance and efficiency of axial-flow turbines under a range of operating situations, with an emphasis on comparing the effects of water and oil as working fluids. Experiments were done with turbines that had 3, 4, and 5 blades at both low (100 rpm) and high (2000 rpm) speeds. We also looked at how oil pre-heating affects things by changing the oil temperature up to 98°C. The results reveal that oil improves the amount of mechanical power and head generated, especially at higher speeds and blade counts. However, it also increases the pressure drop since it is thicker. Pre-heating the oil significantly improves performance, and the 5-blade turbine design may get up to 37% better under the best circumstances. Moderate flow rates and higher oil temperatures provide the best hydraulic efficiency, which shows how important the qualities of the working fluid and the operating conditions are for turbine performance. These results provide useful advice on how to get the most performance out of turbines used in industrial energy recovery.

Index-words: *Axial-flow turbine, Experimental study, Hydraulic efficiency, Blade count, Oil pre-heating, Mechanical power, Pressure drop, Water-oil comparison, Industrial application.*

I. Introduction

Renewable energy technologies currently constitute approximately 34% of the global installed power capacity, totaling around 2,179 GW, with hydropower significantly contributing 1,151 GW or 18% [1, 2]. Given the urgent global challenges related to climate change and rising energy demands, it is essential to expedite the adoption and expansion of renewable energy sources, particularly solar, wind, and hydropower, to achieve substantial reductions in carbon emissions within the coming decade [3]. Additionally, low-head hydropower and hydrokinetic (HK) technologies, which capture energy from flowing water and waves, represent critical components of sustainable energy growth, effectively harnessing untapped renewable resources [4, 5].

According to the International Hydropower Association's 2022 Hydropower Status Report, global hydropower capacity has reached 1,360 GW, growing at an annual rate of 1.9% [6]. However, traditional hydrokinetic turbines, specifically propeller turbines (Kaplan) and Francis turbines, while beneficial for energy production, often involve significant initial investments and substantial civil works. These traditional installations notably contribute to carbon and greenhouse gas emission reductions but pose considerable environmental challenges, such as harm to aquatic ecosystems and water quality degradation [7,8]. Consequently, the renewable energy sector has increasingly shifted focus towards innovative, low-head technologies and unconventional methodologies aimed at minimizing environmental impacts and effectively harnessing very modest head and velocity sources [9].

Vertical axis turbines, specifically cross-flow turbines, encompass two major types: Savonius (drag-based) and Darrieus (lift-based). The distinction between these turbine types lies in their rotational motion mechanisms. Savonius turbines provide significant advantages in low-speed, high-torque scenarios typical of low-head conditions, attributed to their superior torque generation capabilities even at low tip speed ratios [10]. Hybrid turbine models

Volume 11, Issue 2, December 2025 - ISSN 2356-8569
http://dx.doi.org/10.21622/RESD.2025.11.2.1445

combining Savonius and Darrieus configurations successfully integrate the self-starting capability of Savonius turbines and the high maximum power coefficient of Darrieus turbines, though Savonius turbines alone tend to outperform hybrids at very low velocities [11, 12]. Furthermore, given the fluid density differences, hydrokinetic turbines generate significantly higher torque compared to wind turbines with equivalent swept areas [13]. Recent studies on enhanced Savonius rotor designs with aerodynamic improvements demonstrate notable efficiency gains, particularly in low-velocity flow conditions [14, 15].

The design aspects of renewable energy systems, particularly hydrokinetic turbines, require special attention to cost-effectiveness, minimal environmental impact, and high efficiency. Critical design parameters include blade geometry, number of blades, overlap ratios, aspect ratios, twist angles, and end plates [16-22]. Adjusting blade twist angles optimizes three-dimensional flow characteristics, enhancing turbine performance. Innovations such as high-chambered aerofoil blades and spline-shaped geometries further improve efficiency through effective utilization of pressure differentials [23-25]. Additionally, incorporating end plates ensures consistent pressure distribution across blade lengths, significantly improving turbine performance [26-29].

This research evaluates structural enhancements, specifically secondary guide blades and axial spacers, comparing oil and water as working fluids across varying rotational speeds (100 RPM and 2000 RPM) and temperatures. Key parameters assessed include mechanical power output, head increase, efficiency, and pressure drop. The study uniquely integrates fluid pre-heating for improved performance, particularly in industrial applications utilizing waste heat. The primary aim is to determine optimal turbine configurations and operational strategies to maximize efficiency and reduce energy losses. Novel contributions include detailed internal flow modification analysis, fluid type comparisons, and strategic thermal management insights, supporting sustainable and economically viable hydrokinetic turbine development for low-head and industrial energy recovery applications.

II. Methodology

A. Experimental setup

Figures 1a and b present the configuration of the experimental setup designed to evaluate fluid-powered electricity generation. As depicted in Figure 4.1, the system includes a pump that drives the working fluid into a storage tank, where both pressure and liquid level are monitored using appropriate sensors. From the tank, the fluid is directed through a pipeline towards the turbine generator, which converts the fluid's kinetic energy into electrical energy. The setup features pressure sensors at strategic points before and after the turbine to monitor pressure changes. Additionally, a current sensor and LED indicator are incorporated to detect and display electrical output during operation. Figure 1 b provides an actual photograph of the assembled apparatus, highlighting the arrangement of each major component. The pump is positioned at the far left and connected to the vertical storage tank. The flow continues through the main pipe, which houses the turbine and is instrumented with both pressure and electrical measurement devices. The LED visually confirms power generation, while the current and voltage measurement unit precisely records electrical performance. This integrated setup ensures accurate data collection for both fluid dynamic and electrical aspects of the experiment.

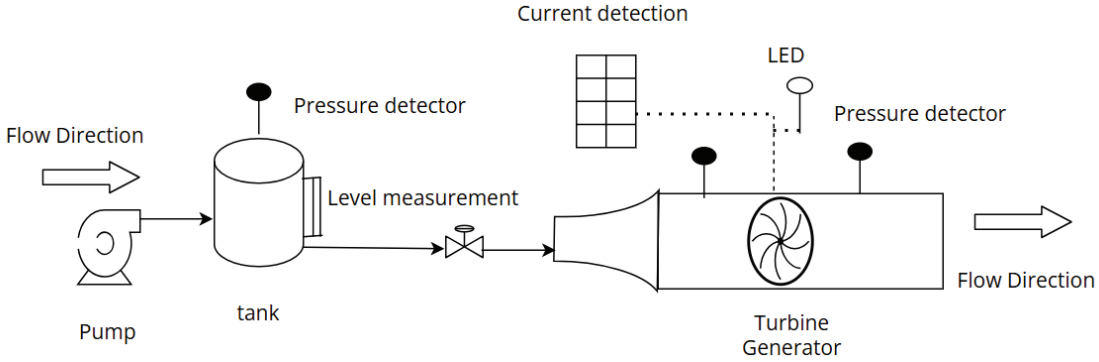

(a) Experimental rig flow sheet

Volume 11, Issue 2, December 2025 - ISSN 2356-8569
http://dx.doi.org/10.21622/RESD.2025.11.2.1445

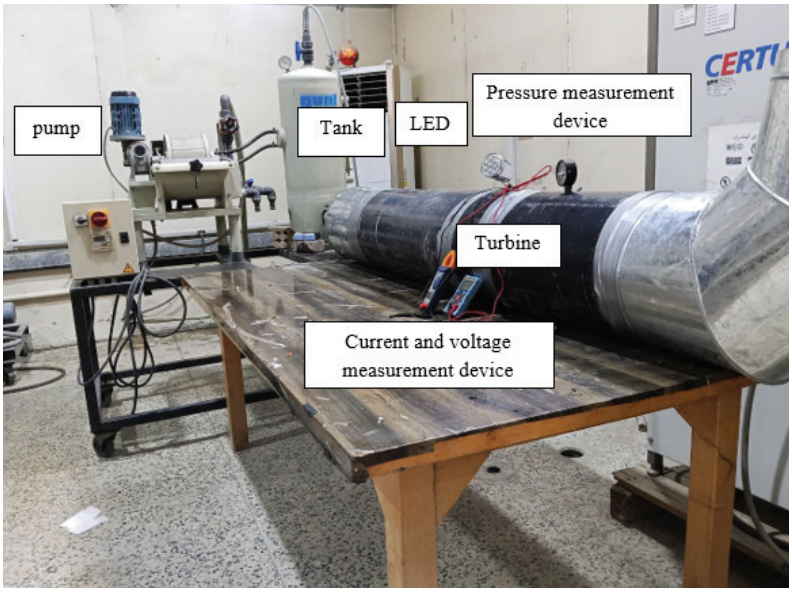

(b) photographic view

Figure 1: Experimental setup of a hydrokinetic turbine.

Figure 2 illustrates the integrated turbine system used for converting the kinetic energy of fluids into electrical energy. The system is primarily composed of a large cylindrical tube made from robust, corrosion-resistant metal—such as aluminum or stainless steel—capable of withstanding high pressures and flow rates. Inside this tube is the main rotating element, typically a large white sphere or disc (the rotor or rotating mass), which is securely mounted on a central shaft with bolts or screws. The design of this turbine is intended to generate flow disturbances as the fluid moves through the pipe. The presence of the internal sphere or disc causes variations in the flow velocity and direction, leading to pressure waves and fluctuations. When the system is in operation, the movement of the fluid pushes the internal mass, causing vibrations or changes in the magnetic field, which are harnessed by a connected generator to produce electricity. Structurally, the turbine ensures that the internal body (either a ball or disc) can move freely or within controlled limits and is designed with sufficient weight to respond appropriately to fluid movement. The internal body is made of materials resistant to corrosion and thermal changes, ensuring long-term durability and stable performance. The image shows a disassembled turbine consisting of four main parts: a front cover, a central cylindrical section, a metallic rotor housing, and a multi-blade rotor. The turbine has a total diameter of 23 cm, with each blade measuring 8 cm in length.

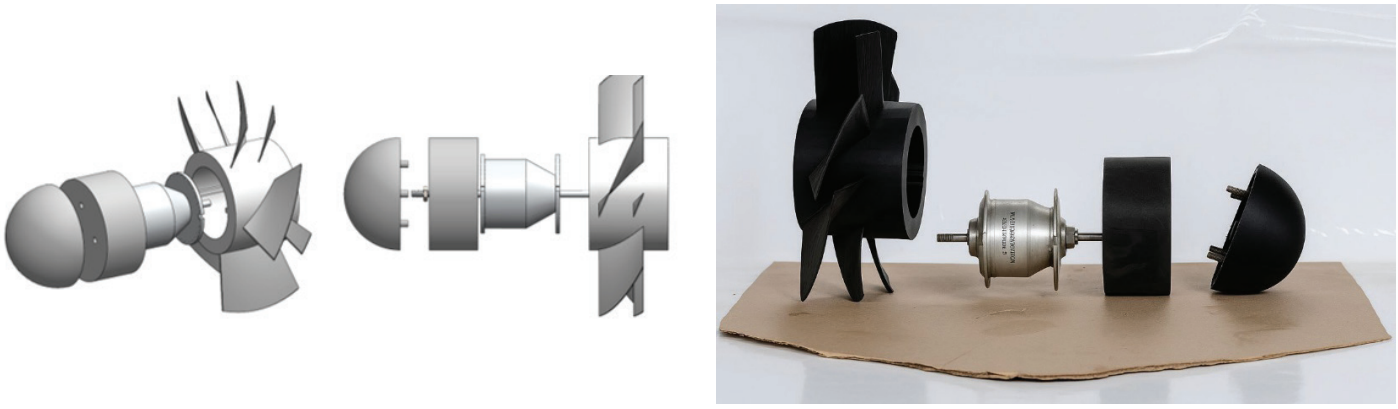

(a) Schematic diagram (b) Photograph view

Figure 2: Turbine impeller and generator.

Volume 11, Issue 2, December 2025 - ISSN 2356-8569
http://dx.doi.org/10.21622/RESD.2025.11.2.1445

B. Experimental procedure

The experimental procedure to assess the hydraulic performance and efficiency of 3, 4, and 5-blade (3B, 4B, and 5B) axial-flow turbine configurations involved a systematic sequence of preparation, operation, and data collection steps. Initially, the entire system—including pump, storage tank, turbine test section, pipes, and measurement instruments—was thoroughly inspected, with all pipe joints securely sealed using high-temperature, leak-resistant insulation tape to prevent leakage. The storage tank was then filled with clean water, ensuring that no air pockets remained by venting the system for continuous, bubble-free flow. All measurement devices, including pressure gauges (WIKA/Atlas Copco) and electrical meters (ZOYI ZT-S1, Eterne VC3267A), were calibrated according to manufacturer guidelines, and the functionality of the LED power indicator was verified. The system was powered up by switching on the control panel and activating the ABB electric motor-driven pump, after which the flow rate was carefully adjusted using throttle valves or pump speed control. The actual flow rate was verified via sight glass or volumetric measurement. After allowing the system to stabilize at each set flow rate, all relevant parameters—including inlet and outlet pressures, tank water level, electrical voltage and current, and LED illumination—were measured and recorded. Each measurement was repeated three times to ensure data repeatability and accuracy. The turbine configuration was then swapped between Configuration 1 and Configuration 4 under identical flow conditions, with all seals and connections re-checked after each change. This process was repeated incrementally for all designated flow rates (0.0049–0.0785 m^3/s), with complete data sets collected at each stage. Upon completion of all tests, the system was gradually shut down, following proper safety protocols to ensure safe power-down and maintenance of the experimental setup.

C. Used Parameters

Table 1 summarizes the key parameters measured and controlled during the experimental evaluation of the turbine system. It provides an overview of each variable, including its symbol, unit of measurement, the method or instrument used for acquisition, the typical range or set value, and a brief description of its role in the study. The parameters include primary hydraulic variables such as flow rate, inlet and outlet pressure, and hydraulic head, all of which are essential for assessing the energy input to the turbine. Additionally, the table lists mechanical and electrical output parameters, including mechanical power, electrical voltage, and current, which are crucial for quantifying system performance and efficiency. The table also notes operational variables such as water temperature and fluid density, which can influence measurement accuracy, as well as the tested turbine configurations.

Table 1: Used parameters in Experimental work

Parameter	Symbol	Unit	Measurement Method	Range / Value
Flow rate	Q	m^3/s	Volumetric (tank method)	0.0049 – 0.0785
Pressure (inlet)	P_{inlet}	kPa / psi	Pressure gauge (WIKA)	0 – 1000 kPa / 0 – 140 psi
Pressure (outlet)	P_{outlet}	kPa / psi	Pressure gauge (WIKA)	0 – 1000 kPa / 0 – 140 psi
Head	H	m	Calculated ($\Delta p/\rho g$)	8 – 18
Mechanical Power	P_{mech}	W	Calculated (ρgQH)	0 – 7000
Electrical Voltage	V	V	Digital multimeter (ZT-S1)	0 – 600
Electrical Current	I	A	Clamp meter (VC3267A)	0 – 10
Efficiency	η	%	Calculated (output/input)	30 – 95
Water temperature	T	°C	Thermometer (if used)	~20–25
Fluid density	ρ	kg/m^3	Assumed/measured	998 (at 20°C)

D. Pre-heater Scenario

In the experimental setup, the oil pre-heating process is implemented by placing a heater directly inside the surge tank, allowing precise control of the oil temperature before it is supplied to the turbine. The heater raises the temperature of the oil to the desired set points, and the actual temperature is monitored

http://dx.doi.org/10.21622/RESD.2025.11.2.1445

and verified using a calibrated thermometer positioned within the tank. This arrangement ensures that the oil enters the turbine at accurately controlled temperatures, enabling a systematic investigation of the effect of thermal conditioning on hydraulic efficiency. By modifying the temperature within the surge tank, the experiment replicates realistic pre-heating scenarios that can be applied in industrial settings, such as refineries, where waste heat or dedicated heating systems can be used to enhance the performance of hydraulic turbines.

Experimental Procedure: Oil Pre-Heater Scenario

1. **Preparation of the Experimental Setup:** Ensure that the hydraulic turbine test rig is properly assembled, with all components including the surge tank, connecting pipelines, pump, flow meter, and the turbine itself correctly installed and leak-free.

2. **Installation of the Heater:** Place an immersion heater inside the surge tank containing the oil. Verify that the heater is compatible with the oil and capable of safely achieving the desired temperature range (e.g., 50°C to 98°C).

3. **Temperature Monitoring:** Position a calibrated thermometer or a digital temperature sensor within the surge tank to continuously monitor the oil temperature. Make sure the sensor is placed at a location that accurately reflects the bulk fluid temperature.

E. Used Calculations

The analysis of the experimental data relied on standard hydraulic and electrical power equations, as well as efficiency calculations, as summarized below:

- Pressure Head (H):

$$H = \frac{\Delta p}{\rho g} \quad (1)$$

Where Δp=pin−pout is the pressure difference across the turbine (Pa), ρ is water density (kg/m^3), and g is gravitational acceleration (9.81 m/s^2).

- Hydraulic Power Input:

$$P_{hyd} = \rho \cdot g \cdot Q \cdot H \quad (2)$$

Where Q is flow rate (m^3/s), H is hydraulic head (m).

- Electrical Power Output:

$$P_{elec} = V \times I \quad (3)$$

Where V is the measured output voltage (V) and I is the current (A).

- Turbine Overall Efficiency (η):

$$\eta = \frac{P_{elec}}{P_{hyd}} \times 100\% \quad (4)$$

expressing the conversion efficiency from hydraulic to electrical power.

F. Accuracy test

Table 2 shows the parameters measured in the experiments with their symbols, units, measurement methods, ranges, and accuracies. The flow rate Q was measured with the volumetric tank method between 0.0049 and 0.0785 m^3/s with an accuracy of about ±0.51%. Inlet and outlet pressures, Pinlet and Poutlet, were taken using WIKA gauges (0–1000 kPa, 1 kPa resolution) with ±0.5% FS (±5 kPa) accuracy. Voltage V was measured by a digital multimeter ZT-S1 (0–600 V, 0.1 V resolution) with ±(0.5% rdg + 2 dgt) accuracy, and current I by a clamp meter VC3267A (0–10 A, 0.01 A resolution) with ±(2% rdg + 5 dgt) accuracy. Temperature T was measured by a thermometer (0–100 °C, 0.1 °C resolution) ±0.5 °C accuracy, and density ρ was assumed/measured 998 ±0.5 kg/m^3 at 20 °C. From these specs, the overall experimental uncertainty was estimated using first-order error propagation, giving:

- **Head, H = Δp/(ρg): ±6%** (dominated by pressure gauge accuracy)
- **Mechanical power, $P_{me}c_h$ = ρgQH: ±6%** (dominated by H)
- **Electrical power, $P_{ele}c$ = VI: ±3.3%**
- **Overall efficiency, η = $P_{me}c_h/P_{ele}c$: ±6.9%**

Where : "% FS" = percent of full scale; "% rdg" = percent of reading; "dgt" = least-significant digits. If your device datasheets list different specs, swap them in, and the propagated accuracies will update accordingly.

Volume 11, Issue 2, December 2025 - ISSN 2356-8569
http://dx.doi.org/10.21622/RESD.2025.11.2.1445

Table 2: Uncertainty values of different parameters

Parameter	Instrument (model)	Range	Resolution	Accuracy
Flow rate, Q (tank method)	Calibrated tank stopwatch	0.0049 – 0.0785 m^3/s	0.001 m^3/s	±0.5% of reading (volume), ±0.01 s (time)
Pressure (inlet/outlet)	WIKA gauge	0–1000 kPa	1 kPa	±0.5% FS (±5 kPa)
Voltage, V	DMM ZT-S1	0–600 V	0.1 V	±(0.5% rdg + 2 dgt)
Currently, I	Clamp VC3267A	0–10 A	0.01 A	±(2% rdg + 5 dgt)
Temperature, T	Thermometer	0–100 °C	0.1 °C	±0.5 °C
Density, ρ (water)	Assumed/measured	—	—	±0.5 $kg·m^{-3}$ (at 20 °C)

III. Results and discussion

A. Comparison between oil and water at low rotation speed (100 rpm)

The comparison between oil and water as working fluids in turbines reveals that oil tends to enhance certain performance parameters, such as mechanical power output and head increase, due to its physical properties. However, this comes at the cost of higher energy losses and pressure drops, suggesting a trade-off that needs to be considered based on the specific operational goals and constraints of the turbine system. These insights are crucial for selecting the appropriate fluid in applications where efficiency and operational cost are critical factors. Figure 3: The graph illustrates a distinct advantage in mechanical power output when using oil over water across all blade configurations. For instance, the 5B model with oil reaches up to 140 W at 0.08 m^3/s, which is about 30% higher than when using water. The increased viscosity and density of oil likely contribute to better energy transfer and turbine performance. Figure 4, similarly, shows that the head increase is more pronounced with oil, particularly noticeable in the 5B model, which achieves nearly 2 m at higher flow rates, compared to 1.5 m with water. This suggests that oil's properties help maintain a higher driving pressure across the turbine blades, enhancing the hydraulic capabilities of the turbine. Figure 5, Efficiency trends show a more complex behavior. While oil generally maintains higher efficiencies across lower flow rates, the curves converge around medium flow rates, indicating that the type of fluid becomes less influential as the flow increases. At higher flows, all models level off, displaying minimal efficiency differences between oil and water. Figure 6, Pressure drop across the turbines is higher with oil, which is expected due to its greater resistance to flow compared to water. The 5B model with oil, for instance, exhibits pressure drops of up to 20 kPa, whereas with water, the maximum is about 15 kPa. This indicates higher energy dissipation in the system, which correlates with the observed increases in mechanical power and head.

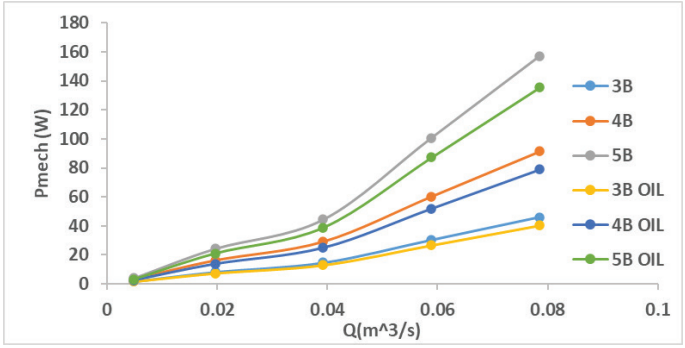

Figure 3: Mechanical power output vs. Flow rate for turbine models using water and oil, 100 rpm.

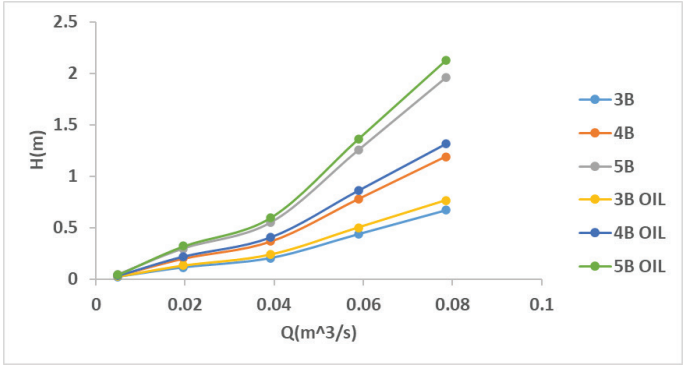

Figure 4: Head increase vs. Flow rate for turbine models using water and oil, 100 rpm.

Volume 11, Issue 2, December 2025 - ISSN 2356-8569
http://dx.doi.org/10.21622/RESD.2025.11.2.1445

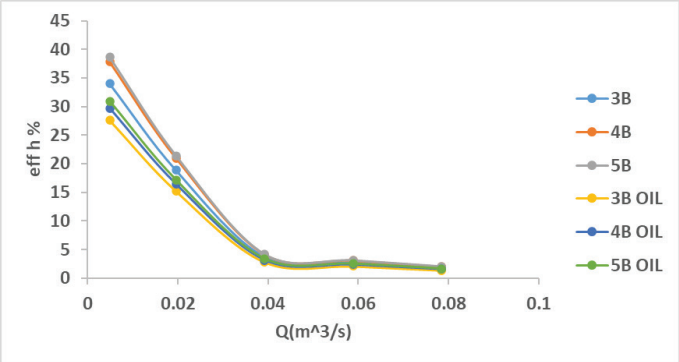

Figure 5: Efficiency vs. Flow rate for turbine models using water and oil, 100 rpm.

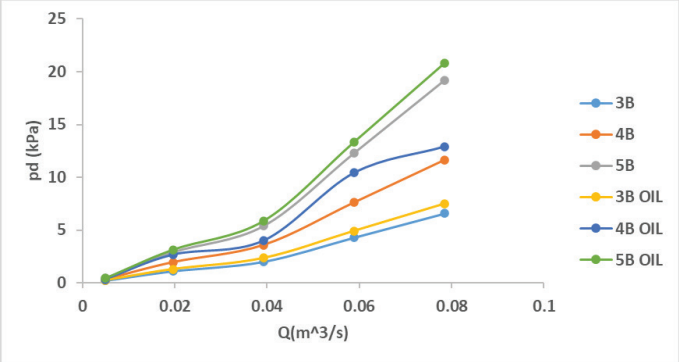

Figure 6: Pressure drop vs. Flow rate for turbine models using water and oil, 100 rpm.

B. Comparison between oil and water at high rotation speed (2000 rpm)

The comparison between 100 RPM and 2000 RPM illustrates that higher rotational speeds amplify the differences between water and oil as turbine fluids. At 100 RPM, the performance differences are less pronounced, likely due to lower shear forces and less impact of fluid viscosity. However, as the RPM increases to 2000, oil's advantages in terms of head generation and mechanical power become more evident, although at the cost of higher energy losses and pressure drops. This behavior underscores the need to choose turbine operating conditions and fluids based on specific performance criteria and efficiency goals, balancing benefits against operational costs.

Figure 7, at 2000 RPM, there is a marked increase in mechanical power output across all blade configurations when using oil compared to water. For example, the 5B model with oil reaches nearly 5500 W at 0.08 m^3/s, significantly higher than water's 3000 W, underscoring oil's superior energy transfer efficiency at high rotational speeds. Figure 8 shows that the increase in head follows a similar trend, with oil producing higher heads at all flow rates. At 2000 RPM, the 5B model with oil achieves over 14 m, compared to just under 10 m with water, highlighting the benefit of using a more viscous fluid under high-speed conditions, which enhances the pressure conversion capability. Figure 9 shows that efficiency at 2000 RPM shows oil maintaining higher values initially, but converges with water as flow increases. Notably, efficiency peaks at around 0.04 m^3/s for all fluids but remains consistently higher for oil, suggesting reduced frictional losses relative to the energy produced. Figure 10, The pressure drop is substantially higher with oil, particularly noticeable in the 4B and 5B models, where it exceeds 120 kPa with oil compared to around 80 kPa with water. This indicates that while oil improves certain performance metrics, it also requires more energy to pump through the system.

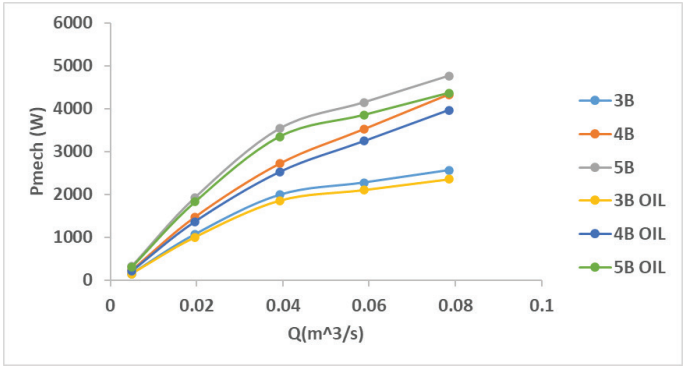

Figure 7: Mechanical power output vs. Flow rate at 2000 RPM for different fluids and blade numbers.

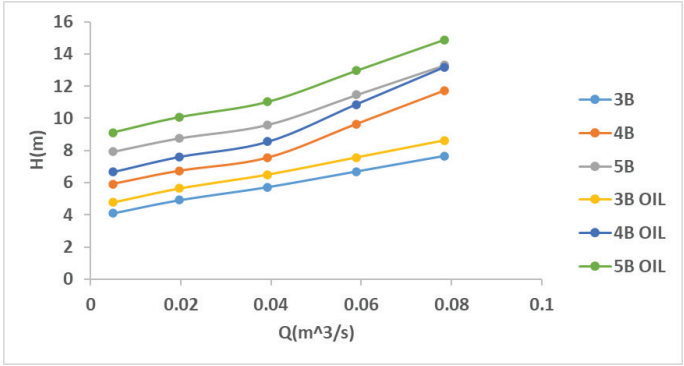

Figure 8: Head increase vs. Flow rate at 2000 RPM for different fluids and blade numbers.

Volume 11, Issue 2, December 2025 - ISSN 2356-8569
http://dx.doi.org/10.21622/RESD.2025.11.2.1445

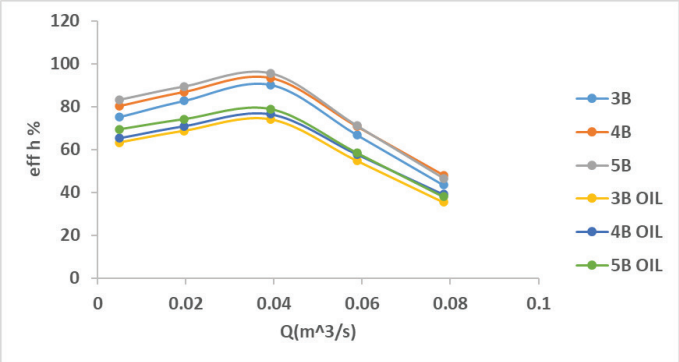

Figure 9: Efficiency vs. Flow rate at 2000 RPM for different fluids and blade numbers.

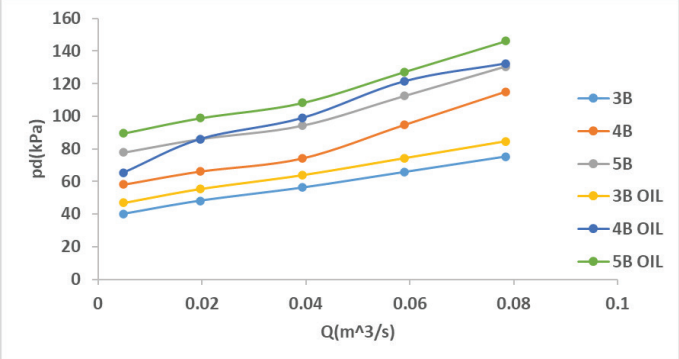

Figure 10: Pressure drop vs. Flow rate at 2000 RPM for different fluids and blade numbers.

C. *Heat map and optimization*

Figure 11 presents a heat map of Overall efficiency for turbines with 3, 4, and 5 blades (3B, 4B, and 5B) across a range of flow rates when water is used as the working fluid. The results clearly show that increasing the number of blades generally leads to higher efficiency, particularly at moderate flow rates. The 5-blade turbine consistently achieves the highest efficiencies, peaking at 95% at a flow rate of 0.04 m^3/s, which can be considered the optimum operating condition for water. At lower and higher flow rates, the efficiency for all configurations declines, but the 5-blade design maintains a significant performance advantage over the 3- and 4-blade options. This suggests that both the number of blades and the flow rate play crucial roles in maximizing the hydraulic efficiency of the system when using water.

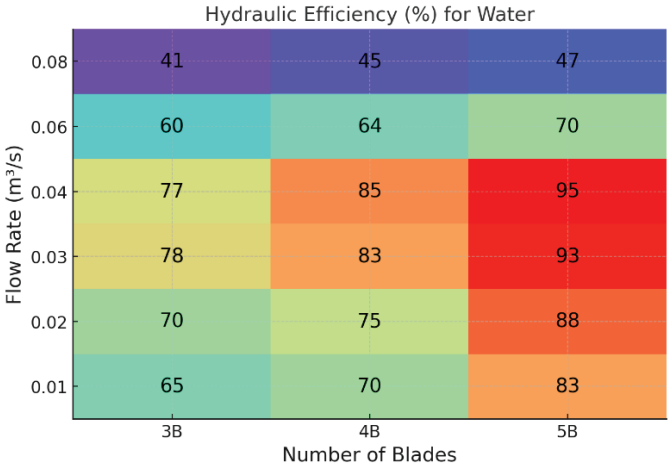

Figure 11: Overall efficiency (%) of turbines with different blade counts (3B, 4B, and 5B) operating under varying flow rates (Q) for both water.

Figure 12 displays the hydraulic efficiency of turbines with 3, 4, and 5 blades operating at varying flow rates, with oil as the working fluid. The overall efficiency values are slightly lower than those observed with water, which can be attributed to the higher viscosity of oil and increased flow resistance. Nevertheless, the same general trend persists: the 5-blade turbine achieves the highest efficiency, reaching a maximum of 79% at a flow rate of 0.04 m^3/s, indicating this as the optimum operational point for oil. At both lower and higher flow rates, the efficiency drops for all blade configurations, with the 5-blade turbine maintaining the best relative performance. These results highlight the importance of optimizing both turbine geometry and operating conditions to achieve maximum efficiency, particularly when dealing with more viscous fluids such as oil.

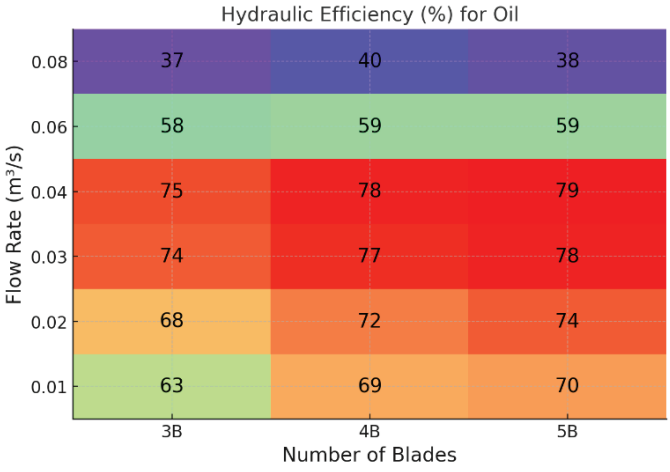

Figure 12: Overall efficiency (%) of turbines with different blade counts (3B, 4B, and 5B) operating under varying flow rates (Q) for both oil.

Volume 11, Issue 2, December 2025 - ISSN 2356-8569
http://dx.doi.org/10.21622/RESD.2025.11.2.1445

D. Pre-heater turbine hydrokinetic

Figures 13-15 clearly demonstrate that oil pre-heating is a robust strategy for improving hydraulic turbine efficiency in refinery scenarios, with the effect amplified by higher blade counts and optimized flow rates. Integrating pre-heating systems using available waste heat is therefore strongly recommended for enhancing the efficiency and sustainability of energy recovery processes in industrial applications.

Across all three figures, a clear trend emerges: increasing the oil temperature from 27°C to 98°C systematically raises the efficiency curves for each blade configuration. This improvement is attributable to the reduction in oil viscosity with higher temperatures, which decreases internal flow resistance and frictional losses within the turbine. As a result, the turbines convert a greater proportion of the available overall energy into useful mechanical work. This finding highlights the value of integrating pre-heating systems in refineries, particularly by utilizing waste heat streams to elevate the working fluid's temperature before turbine entry.

A closer examination of the blade configurations reveals notable distinctions. In Figure 13, representing the 3-blade setup, substantial efficiency gains are observed as temperature increases, with peak efficiency occurring at intermediate flow rates (around 0.03–0.04 m^3/s). However, the efficiency drops sharply at higher flow rates, especially at lower temperatures, indicating greater sensitivity to viscous and turbulent losses. Figure 14, which presents the 4-blade configuration, exhibits similar trends but achieves higher peak efficiencies compared to the 3-blade design. Here, the rise in efficiency with temperature is consistent, and the decline at higher flow rates is slightly less pronounced. In Figure 15, the 5-blade configuration attains the highest overall efficiencies at all tested temperatures. The efficiency peak is broader, and the decline at higher flow rates is less severe, demonstrating the advantages of increased blade count for energy recovery, particularly when combined with oil pre-heating.

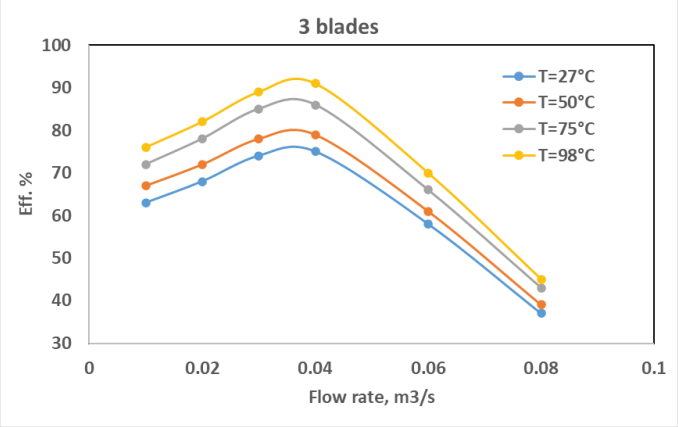

Figure 13: Overall efficiency (%) of turbines with different blade counts 3B operating under varying flow rates (Q) for different temperatures (oil).

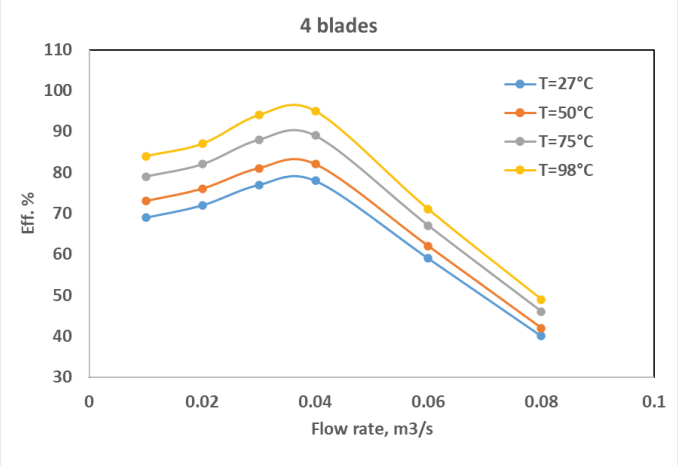

Figure 14: Overall efficiency (%) of turbines with different blade counts 4B operating under varying flow rates (Q) for different temperatures (oil).

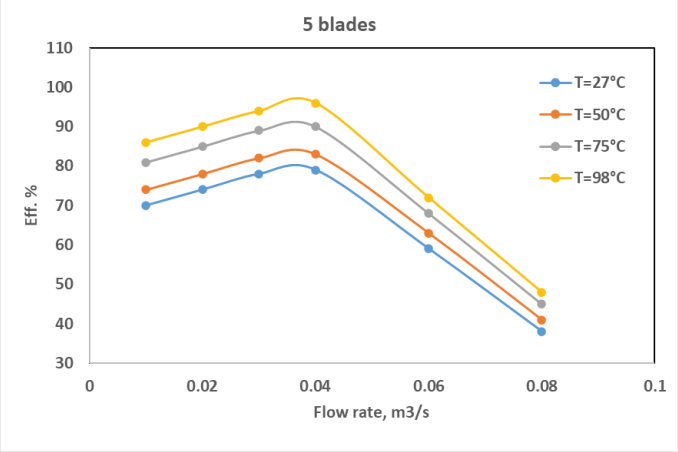

Figure 15: Overall efficiency (%) of turbines with different blade counts 5B operating under varying flow rates (Q) for different temperatures (oil).

Volume 11, Issue 2, December 2025 - ISSN 2356-8569
http://dx.doi.org/10.21622/RESD.2025.11.2.1445

Analysis of the heat maps in Figures 16 through 18 reveals distinct differences in the maximum efficiency enhancement achieved for each blade configuration under varying flow rates and oil temperatures. For the 3-blade turbine (Figure 5.58), the highest efficiency enhancement was **22%**, occurring at a flow rate of 0.08 m^3/s and an oil temperature of 98°C. The 4-blade turbine (Figure 5.59) exhibited a significantly higher maximum enhancement, reaching **33%** at the lowest tested flow rate of 0.01 m^3/s and the highest temperature of 98°C. The most substantial improvement was observed for the 5-blade configuration (Figure 5.60), where the maximum efficiency enhancement attained **37%** under the same optimal conditions of low flow rate (0.01 m^3/s) and elevated oil temperature (98°C). These results clearly demonstrate that increasing the number of blades not only raises the achievable efficiency but also amplifies the positive impact of oil pre-heating, especially at low flow rates and high operating temperatures. This finding underscores the importance of both blade design and thermal management in maximizing turbine performance in refinery applications.

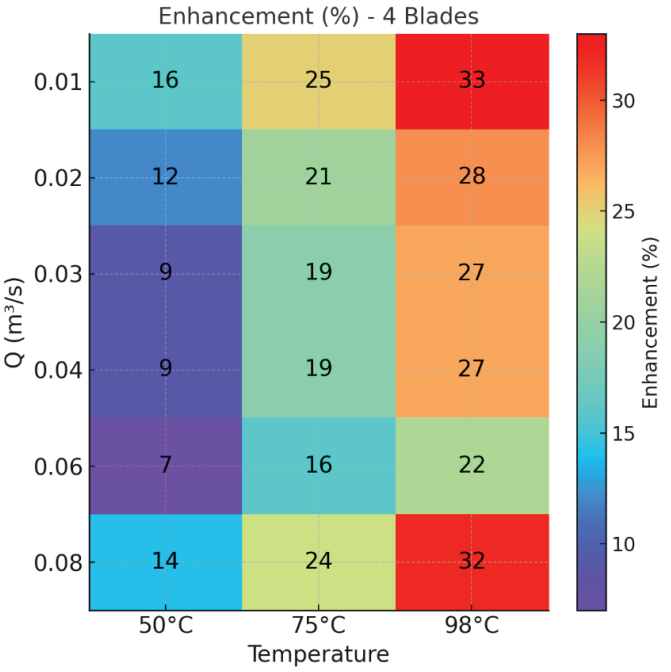

Figure 17: Overall efficiency enhancement (%) of turbines with different blade counts 4B operating under varying flow rates (Q) for different temperatures (oil).

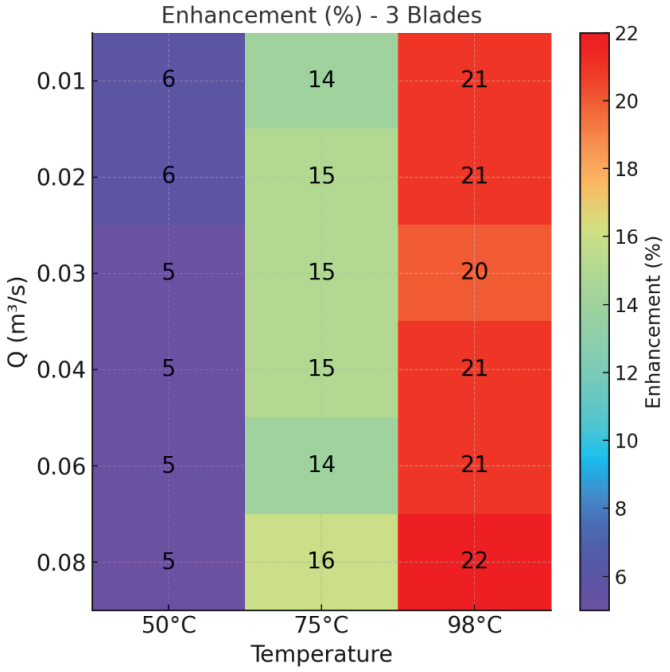

Figure 16: Overall efficiency enhancement (%) of turbines with different blade counts 3B operating under varying flow rates (Q) for different temperatures (oil).

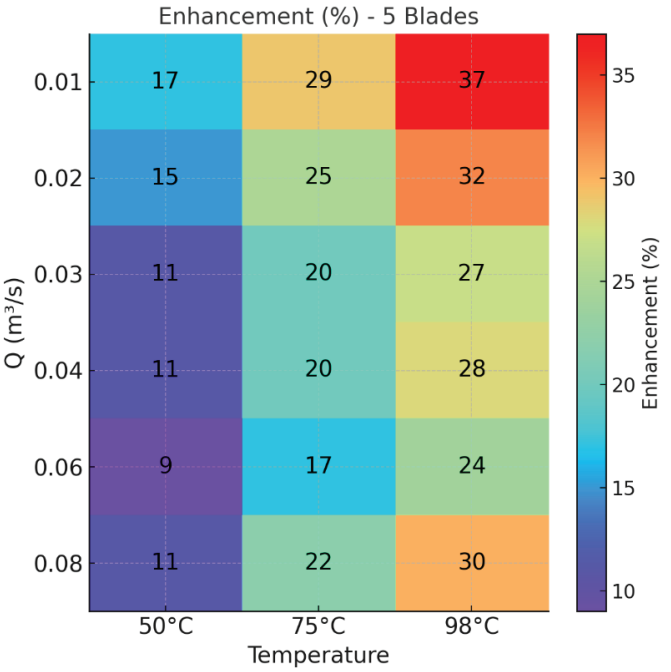

Figure 18: Overall efficiency enhancement (%) of turbines with different blade counts 5B operating under varying flow rates (Q) for different temperatures (oil).

Volume 11, Issue 2, December 2025 - ISSN 2356-8569
http://dx.doi.org/10.21622/RESD.2025.11.2.1445

The influence of flow rate is evident across all figures. Efficiency increases with flow rate up to an optimal point, after which it declines as flow-induced losses become significant. Notably, the optimal efficiency is achieved at higher values and across a broader flow rate range as oil temperature rises, underscoring the enhanced operational flexibility provided by oil pre-heating. From a practical perspective, these results underscore the substantial benefits of using pre-heated oil in refinery turbine systems. Utilizing available process heat to pre-heat oil allows refineries to significantly boost the performance of hydraulic turbines and increase overall power generation. Moreover, higher blade numbers in turbine design further amplify the benefits of oil pre-heating, enabling greater efficiency and operational stability across a wider range of flow rates. Finally, leveraging waste heat for oil pre-heating aligns with sustainable energy practices and improves the overall energy footprint of refinery operations.

The data in **Table 3** provide the physical basis for the performance trends shown in **Figure 18** as temperature increases from 50 °C to 75 °C, the oil's density changes only slightly, while its dynamic viscosity decreases substantially—from approximately 3.0 mPa·s to 1.8 mPa·s. This reduction in viscosity lowers viscous shear losses and internal flow resistance within the turbine passages, resulting in less pressure drop and more effective energy conversion. In **Figure 18**, this behaviour is reflected in the consistent enhancement in performance (%) across all flow rates, with the most pronounced gains occurring at low discharges where viscous effects are dominant—reaching up to 37% at 98 °C and Q = 0.01 m^3/s. At higher flow rates, the influence of viscosity reduction remains beneficial but is moderated by the growing impact of inertial losses. Together, Table 2 and Figure 18 demonstrate that viscosity reduction with temperature is a key driver of turbine efficiency improvements, particularly in low-flow operating regimes.

Table 3: Oil temperature-dependent physical properties

Property	Average Value (50–75 °C)	Units	Notes
Density (ρ)	~820–830	kg/m^3	Slightly decreases with temperature (~0.6 kg/m^3 per °C)
Dynamic viscosity (μ)	~1.8–3.0	mPa·s (cP)	Drops significantly with temperature; actual range depends on crude type

IV. Conclusions

This study presents a comprehensive assessment of axial-flow hydraulic turbines operating with water and oil under various conditions, blade configurations, and pre-heating scenarios. The results reveal several key findings relevant for both research and industrial applications:

1. **Fluid Selection Impact:** Oil as a working fluid consistently delivers higher mechanical power output and head increases compared to water, especially evident at higher rotational speeds (2000 rpm). However, these advantages are accompanied by increased pressure drops and energy losses due to oil's higher viscosity and density. Therefore, the choice between oil and water should be guided by the specific performance priorities—whether the goal is maximizing power output or minimizing operational losses.

2. **Effect of Rotation Speed:** At low rotation speeds (100 rpm), the performance gap between oil and water is moderate, but at higher speeds (2000 rpm), oil's superior properties become much more pronounced. This highlights the importance of matching fluid properties to the operational regime of the turbine for optimal results.

3. **Blade Count Optimization:** Across all scenarios, increasing the number of blades (from 3B to 5B) results in substantial efficiency gains, with the 5-blade configuration delivering the best overall performance for both fluids. This effect is most significant at moderate flow rates, where the 5B turbines with water achieved up to 95% efficiency, and with oil reached up to 79%.

4. **Pre-Heating Advantages:** Pre-heating oil significantly reduces viscosity, leading to noticeable improvements in turbine efficiency and power output. The greatest enhancements were observed with high blade counts and at higher oil temperatures (up to 98°C). For example, the 5B turbine exhibited up to 37% efficiency enhancement at optimal conditions (low flow, high temperature). This underscores the value of integrating waste heat utilization systems in refineries for pre-heating working fluids.

5. **Hydraulic Efficiency Trends:** Hydraulic efficiency peaks at intermediate flow rates and declines at both lower and higher flow rates due to increased frictional and turbulent losses. However, higher oil temperatures and blade numbers expand the range of optimal operation, providing greater flexibility and performance stability.

6. **Energy Sustainability Implications:** Utilizing oil pre-heating by leveraging available waste heat aligns with sustainable industrial practices. It not only boosts turbine efficiency and power generation but also contributes to improving the overall energy footprint of refinery operations.

References

[1] C. M. Niebuhr, M. van Dijk, V. S. Neary, and J. N. Bhagwan, "A review of hydrokinetic turbines and enhancement techniques for canal installations: Technology, applicability and potential," *Renewable and Sustainable Energy Reviews*, vol. 113, p. 109240, Oct. 2019, doi: 10.1016/j.rser.2019.06.047.

[2] M. Bilgili, H. Bilirgen, A. Ozbek, F. Ekinci, and T. Demirdelen, "The role of hydropower installations for sustainable energy development in Turkey and the world," *Renew Energy*, vol. 126, pp. 755–764, Oct. 2018, doi: 10.1016/j.renene.2018.03.089.

[3] IPCC, "Global Warming of 1.5 oC," 2020, *Intergovernmental Panel on Climate Change*. [Online]. Available: https://www.ipcc.ch/sr15/

[4] NREL, "Renewable Electricity Futures Study | Energy Analysis | NREL," 2018. [Online]. Available: https://www.nrel.gov/analysis/re-futures.html

[5] M. J. Sale *et al.*, "Opportunities for Energy Development in Water Conduits: A Report Prepared in Response to Section 7 of the Hydropower Regulatory Efficiency Act of 2013," Oak Ridge, TN (United States), Sep. 2014. doi: 10.2172/1332065.

[6] E. Quaranta, A. Bahreini, A. Riasi, and R. Revelli, "The Very Low Head Turbine for hydropower generation in existing hydraulic infrastructures: State of the art and future challenges," *Sustainable Energy Technologies and Assessments*, vol. 51, p. 101924, Jun. 2022, doi: 10.1016/j.seta.2021.101924.

[7] M. M. Kamal and R. P. Saini, "A review on modifications and performance assessment techniques in cross-flow hydrokinetic system," *Sustainable Energy Technologies and Assessments*, vol. 51, 2022, doi: 10.1016/j.seta.2021.101933.

[8] Y. Chu *et al.*, "Systems Accounting for Carbon Emissions by Hydropower Plant," *Sustainability (Switzerland)*, vol. 14, no. 11, 2022, doi: 10.3390/su14116939.

[9] M. Sood and S. K. Singal, "Development of hydrokinetic energy technology: A review," 2019. doi: 10.1002/er.4529.

[10] E. Quaranta, A. Bahreini, A. Riasi, and R. Revelli, "The Very Low Head Turbine for hydropower generation in existing hydraulic infrastructures: State of the art and future challenges," *Sustainable Energy Technologies and Assessments*, vol. 51, p. 101924, Jun. 2022, doi: 10.1016/j.seta.2021.101924.

[11] J. V. Akwa, H. A. Vielmo, and A. P. Petry, "A review on the performance of Savonius wind turbines," 2012. doi: 10.1016/j.rser.2012.02.056.

[12] G. Saini and R. P. Saini, "A computational investigation to analyze the effects of different rotor parameters on hybrid hydrokinetic turbine performance," *Ocean Engineering*, vol. 199, 2020, doi: 10.1016/j.oceaneng.2020.107019.

[13] T. Alam and M. T. Iqbal, "Design and Development of a Hybrid Vertical Axis Turbine," in *Canadian conference on electrical and computer engineering*, Routledge, 2009, pp. 1178–1183.

[14] A. S. Bahaj and L. E. Myers, "Fundamentals applicable to the utilisation of marine current turbines for energy production," *Renew Energy*, vol. 28, no. 14, 2003, doi: 10.1016/S0960-1481(03)00103-4.

[15] C. M. L. Song and M.-Z. Zhang, "Performance study for a novel vertical axis wind turbine based on simulation analysis," in *IEEE 14th International Conference on Networking, Sensing and Control (ICNSC)*, 2017, pp. 549–554.

[16] S. J. Savonius, "Rotor adapted to be driven by wind or flowing water," *Patient*, 1929.

[17] A. S. Saad, I. I. El-Sharkawy, S. Ookawara, and M. Ahmed, "Performance enhancement of twisted-bladed Savonius vertical axis wind turbines," *Energy Convers Manag*, vol. 209, 2020, doi: 10.1016/j.enconman.2020.112673.

[18] A. Damak, Z. Driss, and M. S. Abid, "Experimental investigation of helical Savonius rotor with a twist of 180°," *Renew Energy*, vol. 52, 2013, doi: 10.1016/j.renene.2012.10.043.

[19] I. Ross and A. Altman, "Wind tunnel blockage corrections: Review and application to Savonius vertical-axis wind turbines," *Journal of Wind Engineering and Industrial Aerodynamics*, vol. 99, no. 5, 2011, doi: 10.1016/j.jweia.2011.02.002.

[20] R. E. Sheldahl, B. F. Blackwell, and L. V. Feltz, "WIND TUNNEL PERFORMANCE DATA FOR TWO- AND THREE-BUCKET SAVONIUS ROTORS.," *J Energy*, vol. 2, no. 3, 1978, doi: 10.2514/3.47966.

[21] M. H. Mohamed, G. Janiga, E. Pap, and D. Thèvenin, "Optimization of Savonius turbines using an obstacle shielding the returning blade," *Renew Energy*, vol. 35, no. 11, 2010, doi: 10.1016/j.renene.2010.04.007.

[22] U. K. Saha, S. Thotla, and D. Maity, "Optimum design configuration of Savonius rotor through wind tunnel experiments," *Journal of Wind Engineering and Industrial Aerodynamics*, vol. 96, no. 8–9, 2008, doi: 10.1016/j.jweia.2008.03.005.

[23] W. A. El-Askary, A. S. Saad, A. M. AbdelSalam, and I. M. Sakr, "Investigating the performance of a twisted modified Savonius rotor," *Journal of Wind Engineering and Industrial Aerodynamics*, vol. 182, 2018, doi: 10.1016/j.jweia.2018.10.009.

[24] M. Tartuferi, V. D'Alessandro, S. Montelpare, and R. Ricci, "Enhancement of savonius wind rotor aerodynamic performance: A computational study of new blade shapes and curtain systems," *Energy*, vol. 79, no. C, 2015, doi: 10.1016/j.energy.2014.11.023.

[25] K. Kacprzak, G. Liskiewicz, and K. Sobczak, "Numerical investigation of conventional and modified Savonius wind turbines," *Renew Energy*, vol. 60, 2013, doi: 10.1016/j.renene.2013.06.009.

[26] P. K. Talukdar, A. Sardar, V. Kulkarni, and U. K. Saha, "Parametric analysis of model Savonius hydrokinetic turbines through experimental and computational investigations," *Energy Convers Manag*, vol. 158, 2018, doi: 10.1016/j.enconman.2017.12.011.

[27] V. Uniyal, A. Karn, and V. P. Singh, "Parametric optimization of Archimedes screw turbine by response surface methodology and artificial neural networks," *Renewable Energy and Sustainable Development*, vol. 10, no. 2, p. 306, Oct. 2024, doi: 10.21622/resd.2024.10.2.1008.

[28] P. Dhiman, V. P. Singh, and A. Karn, "Experimental and computational analysis of air injection as a mitigation technique for silt erosion in hydro turbines," *Renewable Energy and Sustainable Development*, vol. 10, no. 2, p. 345, Nov. 2024, doi: 10.21622/resd.2024.10.2.1054.

[29] W. M. L. Monteiro, A. Sarmento, B. Semedo, A. Carvalho, T. Tavares, and J. A. L. Monteiro, "Utilizing maritime caves for wave energy: wells turbine performance and household power supply from cave-generated electricity," *Renewable Energy and Sustainable Development*, vol. 10, no. 2, p. 384, Nov. 2024, doi: 10.21622/resd.2024.10.2.1019.